Thin Solid Films 519 (2011) 2811–2816

Contents lists available at ScienceDirect

Thin Solid Films

journal homepage: www.elsevier.com/locate/tsf

Band alignment of metal-oxide-semiconductor structure by internal photoemission spectroscopy and spectroscopic ellipsometry

N.V. Nguyen *, O.A. Kirillov, J.S. Suehle

Semiconductor Electronics Division, National Institute of Standards and Technology, Gaithersburg, MD 20899, United States

ARTICLE INFO

Available online 10 December 2010

Keywords:
Internal photoemission
Spectroscopic ellipsometry
High-k dielectric
Metal gate
MOS
Band offsets
Band alignment
Interface

ABSTRACT

In this paper, we will provide an overview of the internal photoemission (IPE) and the significance of this technique when combined with spectroscopic ellipsometry (SE) to investigate the interfacial electronic properties of heterostructures. In particular, the main interest is focused on the electron transport mechanism and properties at and near the interface of the technologically important metal-oxide-semiconductor (MOS) devices. Not until recently, IPE and SE have become important metrology tools in band offset characterization for the MOS materials. The most common and straightforward application of IPE and SE is to determine how the Fermi level of the metal, and the conduction and valence bands of the semiconductor align with those of the oxide of the MOS structure. For demonstration, we will present the results recently obtained on a set of MOS devices consisting of metal gate / high-k dielectric stack / Si and III–V high mobility substrate. The examples include [TaN/TaSiN] metal gate / [HfO_2/SiO_2] dielectric stack / Si substrate and Al metal gate / Al_2O_3 dielectric / $In_xGa_{1-x}As$ substrate.

Published by Elsevier B.V.

1. Introduction

One of the more important parameters that need to be known and/or controlled in order to fabricate high performance electronic devices is the electron and hole barrier heights at the interfaces. In particular for the field of complementary metal oxide semiconductor (CMOS), there has been very active research to find new materials to replace the traditional *poly*-Si gate / SiO_2 / Si structure of the basic MOS for the next generations of CMOS devices. As the gate lengths of the metal-oxide-semiconductor field-effect transistor (MOSFET) are reduced to below 50 nm and associated scaling of the dielectrics thickness continues, a number of performance issues such as high leakage current and *poly*-Si electrode depletion are encountered. To circumvent these problems, both SiO_2 and *poly*-Si gate need to be replaced with appropriate high-*k* dielectrics and metal gates. Furthermore, high-mobility III–V compound semiconductor channel materials coupled with a high-*k* gate dielectric have recently become a major focus as a possible technology to support the further scaling of the advanced MOSFET technology [1]. One of the critical electronic parameters that greatly affects the device performance is the interfacial band offset. For instance, to replace SiO_2 with a high-*k* dielectric in silicon-base MOSFET devices, both valence and conduction band offsets of the material are required to be greater than 1 eV with respect to the silicon band edges [2]. Therefore, it is highly desirable to be able to measure directly the band offsets at the interfaces of a MOS device. Recently, IPE has been shown to be a simple yet robust and powerful technique for characterizing electronic properties of solid-solid interfaces, in particular those of insulator/semiconductor and metal/insulator [3].

In this article, a brief introduction to IPE with an emphasis on threshold spectroscopy is presented. To obtain a complete band alignment picture, vacuum ultraviolet spectroscopic ellipsometry (VUV-SE) is used as a complementary technique to measure the band gaps of high-k dielectric of the MOS structure. The VUV-SE spectral range extended into the vacuum ultraviolet region is usually required since the band gaps of most common high-k dielectrics are greater than about 5 eV. We will combine these two techniques to examine the electronic interface properties of a technologically important class of MOS which includes [TaN/TaSiN] metal gate / [HfO_2/SiO_2] dielectric stack / Si and Al metal gate / Al_2O_3 dielectric / $In_xGa_{1-x}As$ substrate.

2. Internal photoemission as threshold spectroscopy

IPE is defined as a process where photon-stimulated charge carriers (electrons and/or holes) make the transition from one component (emitter) of a hetero-structure to another (collector) over the energy barrier height at their interface. In effect, the process involves photo-generating carriers in the emitter, transporting them to the interface, and transferring sufficient energy to the carriers for them to escape over the barrier to become carriers in the collector. These carriers are then subjected to an external potential to produce

* Corresponding author.
E-mail address: nhan.nguyen@nist.gov (N.V. Nguyen).

0040-6090/$ – see front matter. Published by Elsevier B.V.
doi:10.1016/j.tsf.2010.11.080

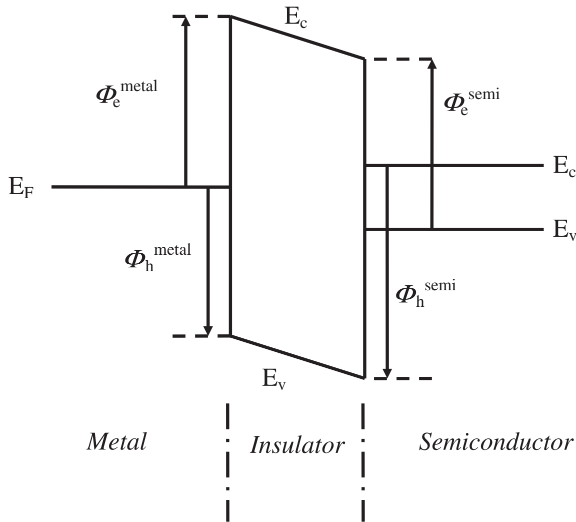

Fig. 1. Schematic energy band diagram of a MOS structure with all barrier energy indicated.

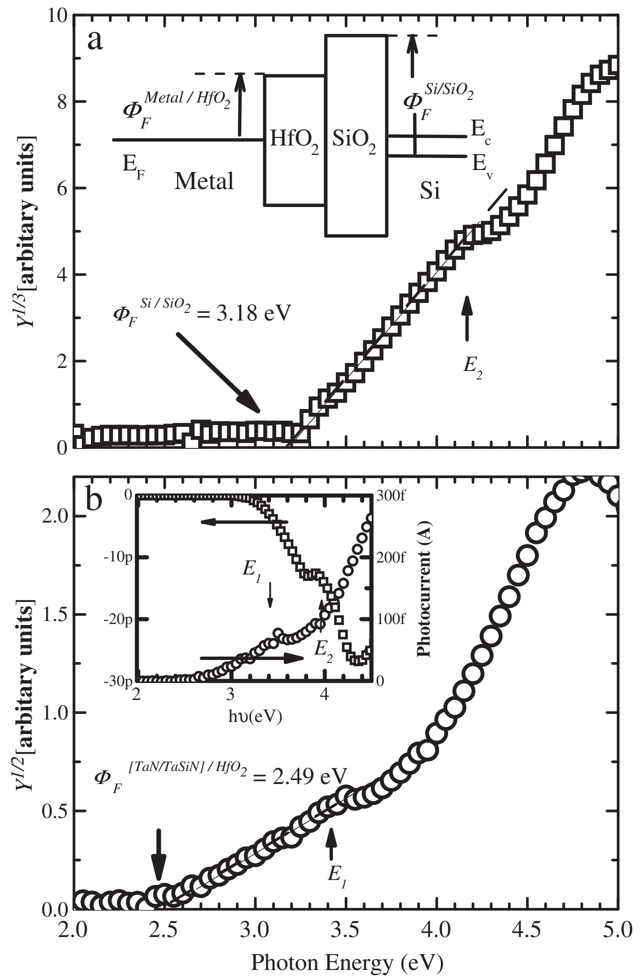

Fig. 2. Typical IPE responses of [TaN/TaSiN] stack / [HfO_2/SiO_2] stack / Si for an average electric field of 3.6 MV/cm in the dielectric stack. Determination of barrier height at (a) Si and [HfO_2/SiO_2] stack interface and (b) [TaN/TaSiN] stack and [HfO_2/SiO_2] stack interface. The inset is the magnitude comparison of photocurrents ejected from Si (left axis) and from [TaN/TaSiN] stack (right axis) over the [HfO_2/SiO_2] stack. Energy band schematic (not to scale) is simply to illustrate the barriers measured in (a) and (b).

photocurrents. In order for the photoemission yield, i.e. the ratio of photocurrent and incidence photon intensity, to be correctly measured, the carrier trap density should be sufficiently small so to not distort the internal electric field. In other words, the insulator thickness should be comparable or less than the mean free path length of the carriers [4]. Furthermore, this description of IPE has neglected the possible tunneling of the photo-excited charge carriers through the barrier in the energy range below the barrier height. Although the tunneling can be taken into account, its effects on the barrier height threshold determination was found to be negligible under the electric field strength commonly used in IPE experiments [5]. As a threshold measurement, the onset of the conduction of these photoemission carriers under the incidence of certain minimum photon energy signifies the energy barrier height of the same energy.

For a MOS structure, the barrier heights are shown schematically in the energy band diagram in Fig. 1. Φ_e^{metal} and Φ_e^{semi} are the barrier heights for electrons making the transition from the metal Fermi level and the top valence band of the semiconductor to the bottom conduction band of the insulator, respectively. For the hole carriers, Φ_h^{metal} and Φ_h^{semi} are the barrier height from the metal Fermi level and the bottom conduction band of semiconductor to the top valence band of the insulator, respectively. For a typical measurement, IPE used as threshold spectroscopy can accurately measure Φ_e^{metal} and Φ_e^{semi}. Experimentally, to facilitate the described IPE process, the MOS structure is illuminated through a semitransparent thin metal, an external bias (V) is applied between the electrode (metal gate) and the semiconductor substrate, and the photocurrent (I) is measured.

To analyze the photoemission process, the optical excitation and transport processes are characterized by the energy distribution function of the photoemission carriers $N(E, h\upsilon)$ where E is the carrier energy and $h\upsilon$ photon energy and the probability $P(E)$ of the carriers to escape over the barrier. The internal photoemission yield $Y(h\upsilon)$ can be obtained by integrating the product of $N(E, h\upsilon)$ and $P(E)$ over the spectrum of the carrier energy E at the interface. If only carriers in the emitter having the minimum barrier energy (Φ) at the interface are able to transfer to the collector, the yield can be written as $Y(h\upsilon) = A[h\upsilon - \Phi]^p$ where p depends on the energy distribution characteristics of the carriers at the interface and A is a proportionality constant. For the metal/insulator interface with the excitation photon energy near and above Φ, Y has been found to have cubic dependency [6], i.e. $p = 2$, whereas $p = 3$ for the semiconductor/insulator interface [7]. Thus, Φ at the metal/insulator interface and the semiconductor/insulator interface can be experimentally determined by linear extrapolation of the measured $Y^{1/2}$ and $Y^{1/3}$ to zero yield, respectively.

Experimentally, it is rather complicated to measure the internal yield directly because it is difficult to determine the absolute photon flux absorbed in the emitter. In principle, the absolute absorbance in the emitter could be deduced if the reflectance, transmittance, and collector absorption were also measured. This method may be, however, conceivably difficult to realize experimentally because of the geometrical complexity of the sample that may render the reflectivity and transmission measurements impossible to a desired accuracy. Therefore, in practice the external quantum yield Y is commonly employed and defined as:

$$Y = \frac{I.h\upsilon}{P} \tag{1}$$

where I is the photocurrent, P the incident light power and $h\upsilon$ the photon energy. Such an approach works well with most MOS structures used in IPE where the metal plasma frequency lies outside the IPE spectral range and has no optical critical transitions that might give rise to the ambiguity in the determination of the barrier threshold. In addition, the thickness of the collector and emitter of common MOS structures are small compared with the probing

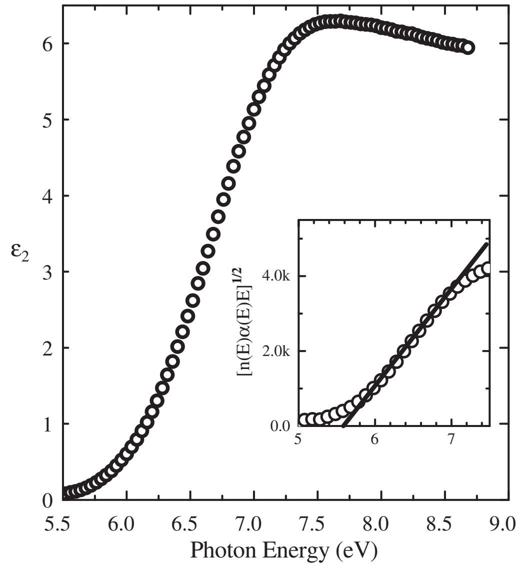

Fig. 3. The imaginary part (ε_2) of the dielectric function of HfO_2 measured by VUV-SE. The inset is the Tauc–Plot from which the band gap is determined.

wavelength so optical interference is avoided. Of course, one should recognize those effects when these conditions are not applicable.

The barrier height is also influenced by the strength of the electric field at the interface. For low and moderately doped semiconductors, the barrier heights can be affected by the image force (Schottky effect), the scattering within the image field, and the traps in the collector [4]. The field-induced lowering of the barrier height or the Schottky effect can be easily shown as [8]:

$$\phi(F) = \phi_0 - q\sqrt{\frac{qF}{4\pi\varepsilon_0\varepsilon_i}} \tag{2}$$

where Φ_0 is the zero-field barrier height, q the electron charge, ε_0 the vacuum permittivity, ε_s the relative permittivity of the insulator, and F is the electric field. Therefore, the *zero*-field barrier height Φ_0 is determined from the Φ vs. $\sqrt{F}$ plot when $F=0$.

3. Experiments and data analysis

The IPE system used in this study consists of a 150 W broadband Xenon light source used in conjunction with a quarter-meter Czerny–Turner, f/4, 1200 line/mm ruled monochromator to provide a spectral range from 1.5 eV to 5.0 eV. High order dispersion is filtered out with two long pass filters. Light from the monochromator is collimated by an achromatic UV-grade lens and then focused down to a millimeter size spot on the metal electrode surface of a MOS device by another achromatic UV-lens of 1 cm focal length. The second lens is auto-adjusted to position the focal point on the surface of the device for each incident photon energy. The bias applied across the MOS capacitor is supplied by a regulated power supply, and the current is recorded by an electrometer as the light is scanned at different photon energies. The quantum yield, Y in Eq. (1), is obtained through the measured photocurrent I normalized *by* the incident light power. For simplicity, the light incident at the surface is used and measured by a calibrated silicon diode right at the focal point of the second lens. All the measured currents are corrected for stray light and possible tunneling and background noise current. Normal operation is usually done by measuring photocurrent as a function of the incident photon energy at an applied bias, and then repeated for a wide range of biases where the tunnel currents are minimal.

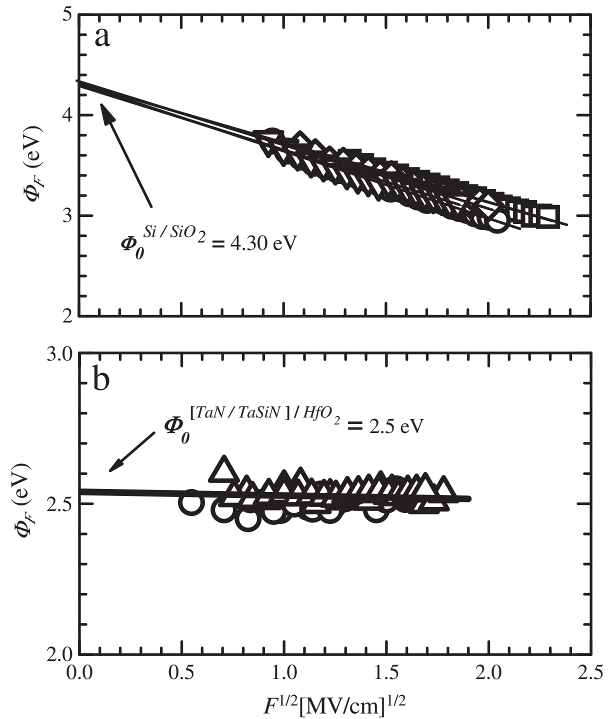

Fig. 4. Schottky plots of barrier height at the Si / SiO_2 interface (a), and the metal stack electrode / HfO_2 interface (b) for [TaN/TaSiN] stack / [HfO_2/SiO_2] stack / Si with various thickness of SiO_2 (squares for 4 nm, circles for 6 nm, and triangles for 8 nm).

Vacuum ultra-violet spectroscopic ellipsometry (VUV-SE) measurements were performed on a commercial J. A. Woollam[1] ellipsometer with the spectral range from 1.0 eV (1240 nm) to 8.7 eV (143 nm). The band gaps reported in this study for the dielectric layer between the semiconductor substrate and the metal gate were determined on a structure without the metal gate on top. Both the layer thickness and the complex dielectric function, $\varepsilon = \varepsilon_1 + i\varepsilon_2$, were obtained from the ellipsometry data by a modeling technique reported elsewhere [9]. The band gap (E_g) of the dielectric was then determined from the energy dependence of its absorption coefficient, $\alpha = 4\pi k/\lambda$, near its absorption edge, where λ is the photon wavelength and k is the extinction coefficient which can be calculated from the relation $(n+ik)^2 = \varepsilon_1 + i\varepsilon_2$ with n being the index of refraction. The most commonly used method to determine E_g for amorphous materials is to use the Tauc plot which shows that near the absorption edge the quantity $[n(E)\alpha(E)E]^{1/2}$ varies linearly with $(E - E_g)$ where E is the photon energy. E_g is thus experimentally obtained by fitting $[n(E)\alpha(E)E]^{1/2}$ to a linear line in the spectral range near the band gap [10].

4. Results and discussion

In the following, IPE and SE data and results are presented for two types of MOS: [TaN/TaSiN] metal gate / [SiO_2/HfO_2] dielectric stack / Si substrate and Al metal gate / Al_2O_3 dielectric / $In_{1-x}Ga_xAs$ substrate. All the dielectrics were grown by atomic layer deposition (ALD). We focus on how IPE is used to determine the barrier heights at material interfaces. The descriptions and in-depth discussion of these materials have been reported somewhere else [11,12].

[1] Certain commercial equipment, instruments, or materials are identified in this paper in order to specify the experimental procedure adequately. Such identification is neither intended to imply recommendation or endorsement by the National Institute of Standards and Technology, nor is it intended to imply that the materials or equipment identified are necessarily the best available for the purpose.

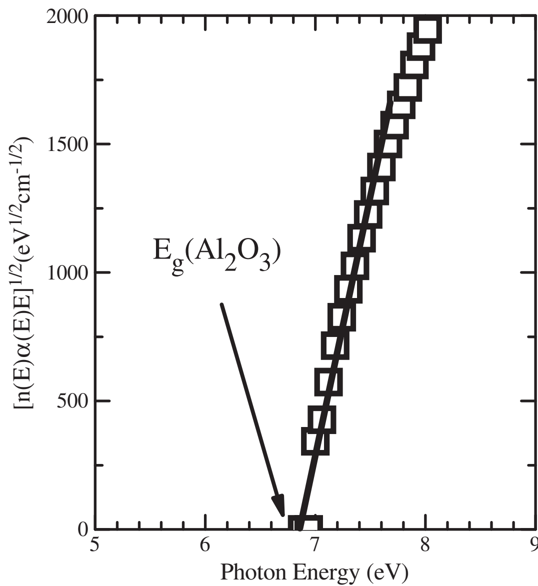

Fig. 5. Tauc–Plot of Al_2O_3 from which the band gap is determined.

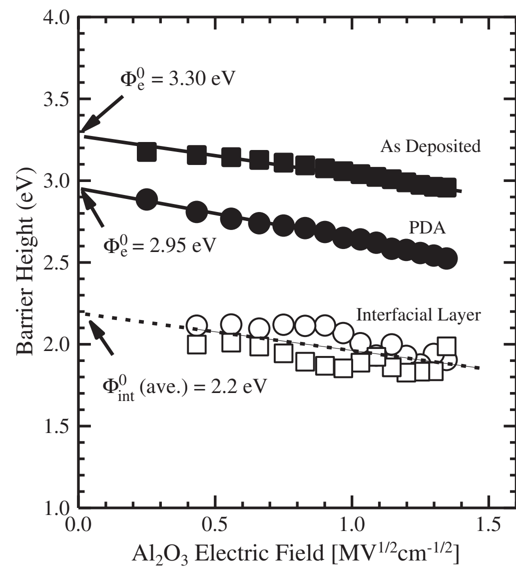

Fig. 7. Schottky plots showing oxide field dependence of the barrier heights at the Al_2O_3/ InGaAs interface for as-deposited and *PDA* Al_2O_3. Φ_e^0's and Φ_{int}^0 are the averaged *zero-field* barrier heights at Al_2O_3/ InGaAs and for the interlayer, respectively.

In Fig. 2 we present the IPE results for a complicated structure where the compound metal was used but the insulator is a stack composed of a HfO_2 layer of 6 nm on a SiO_2 layer of varying thickness of 4 nm, 6 nm, and 8 nm (See the inset of Fig. 2a). Near the threshold, both $Y^{1/2}$ and $Y^{1/3}$ vary linearly with photon energy. Since the conduction band of HfO_2 is about 1 eV lower than that of SiO_2 (based on their electron affinities), the photoelectron injection from the metal gate is controlled by the barrier at the metal and HfO_2 interface. Fig. 2a and b shows, for an average electric field of 3.6 MV/cm, $\Phi_F^{Si/SiO_2} = 3.18$ eV $\pm$ 0.05 eV and $\Phi_F^{[TaN/TaSiN]/HfO_2} = 2.49$ eV. The E_1 and E_2 optical excitations of silicon were also observed to decrease the photoelectron yields. The reduction is due to the strong absorption or

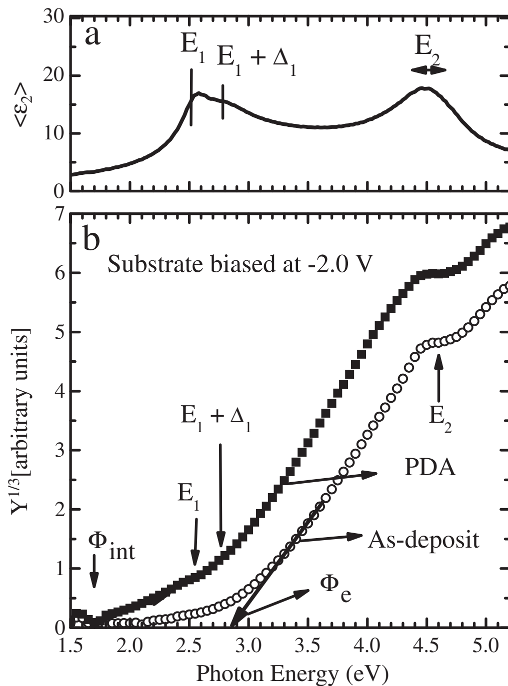

Fig. 6. (a) Imaginary part $<\varepsilon_2>$ of the pseudo-dielectric function of $In_{0.75}Ga_{0.25}As$; (b) Cube root of the typical IPE yield as a function of photon energy where filled and open symbols are for post-deposition-annealed (*PDA*) and as-deposited Al_2O_3. All the IPE data shown were taken with the substrate biased at +2.0 V.

the decreasing light penetration depth and the critical point final state of the transition in the crystal momentum direction being well below the SiO_2 bottom conduction band [4]. From the measured photocurrents shown in the inset of Fig. 2b, we observed that, when the electrons are injected from the metal stack over the HfO_2/SiO_2 two-layer stack, the photocurrents are much lower than when they are injected from Si over the SiO_2/HfO_2 stack for the similar electric field strength in the opposite direction. A likely explanation for this phenomenon is that, in addition to the possible scattering energy losses, trapping, and backward hopping, the effective electron escape probability is further reduced at the HfO_2 and SiO_2 interface after overcoming the first barrier at the metal gate and HfO_2. Fig. 3 displays the imaginary part (ε_2) of the dielectric function of HfO_2 determined from VUV-SE measurement with the inset showing the Tauc–Plot from which the band gap (E_g) of 5.6 eV was extracted by a linear fit. Experimental and theoretical works have already reported on the HfO_2 band gap, giving the values between 5.1 eV and 6.3 eV (see [13] for example). The variations appear to relate to the methods of depositions/growths and experimental techniques used to obtain the band gap. Our value, however, is found to be consistent with those measured by optical methods [9,14]. In addition, the dielectric function containing no absorption features (see Fig. 3) at 0.2–0.3 eV below the optical band gap as seen for poly-crystalline HfO_2 is indicative of an amorphous state [9].

A range of bias from −4.0 V to +4.0 V in steps of 0.2 V was applied and the thresholds were similarly determined for each bias. The same procedure was then repeated for all different thicknesses (4 nm, 6 nm, and 8 nm) of SiO_2. All barrier heights so determined and displayed in the Schottky plots in Fig. 4a and b (see the caption for SiO_2 thickness specifications) approximately follow the same linear field dependence and have a similar magnitude. Thus, the *zero-field* barrier height (Φ_0) at the SiO_2 / Si interface was extracted from all Φ_0's, resulting in an average value of 4.3 eV, which is expected to be the same as in the case of a single SiO_2 dielectric layer [15]. It is worth noting that the SiO_2 layer is relatively thick so that the band offset between Si and HfO_2 was not directly extracted as opposed to the case where the interlayer between Si and HfO_2 is much thinner. In an example of the latter, Afanas'ev et al. have shown that IPE-determined barrier height between HfO_2 and Si is independent of the type of the interlayer (Si_2N_4, SiON, and SiO_2) which they suggested the dipole contribution

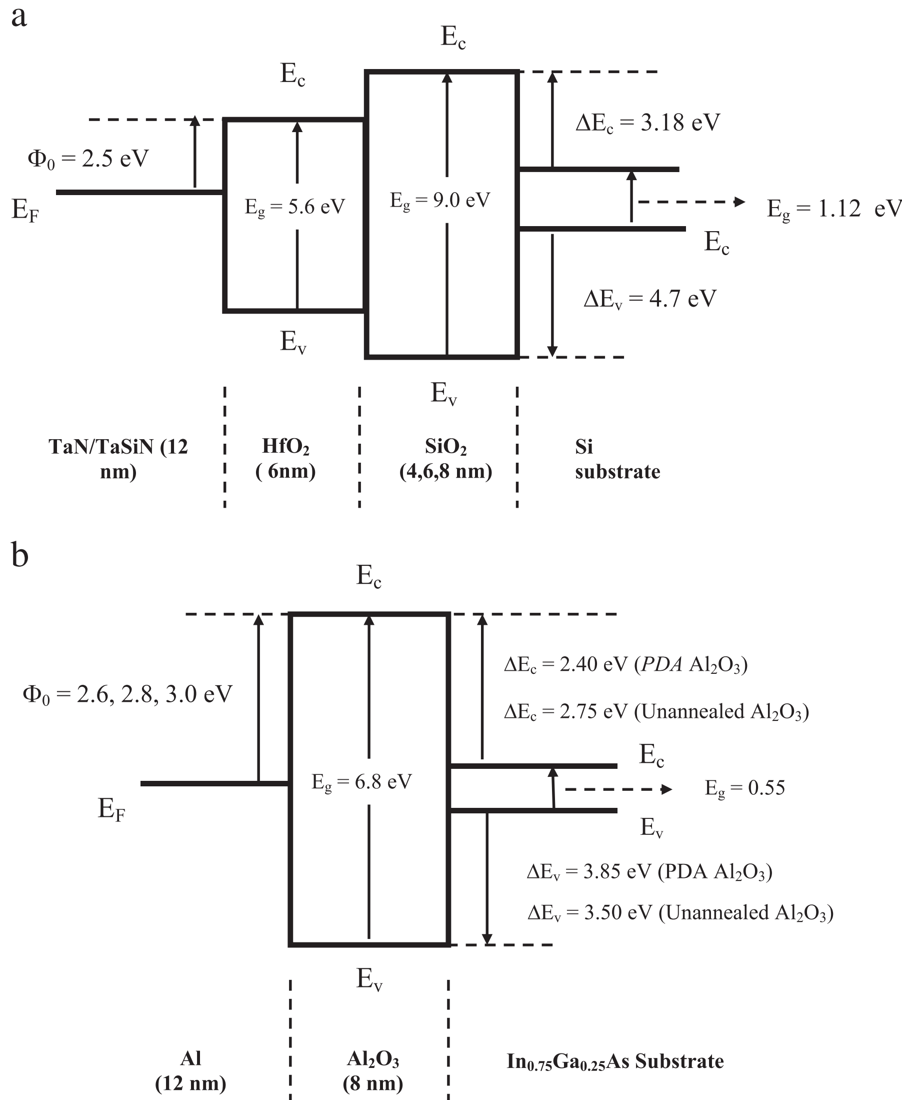

Fig. 8. Schematic diagrams (not to scale) showing the band offsets of (a) [TaN/TaSiN] stack / [HfO_2/SiO_2] stack / Si and (b) Al / Al_2O_3 / $In_{0.75}Ga_{0.25}As$. All the layer thicknesses are indicated next to the material symbols.

of these interlayers to the barrier height is negligible [16]. From Fig. 4b, at the [TaN/TaSiN] / HfO_2 interface, the determined average barrier height value was found to be similar and to scatter within 0.1 eV around 2.5 eV. Furthermore, the barrier height appears insensitive to the electric field in the insulators. This can be attributed to the higher permittivity of HfO_2, electron scatterings, and to the effect of the possible negative plane charges existing in the insulator near the interface with the metal [7]. Such a plane charge creates a Coulomb potential which can screen the influence of the external field on the carriers in the oxides. Similar weak field induced barrier lowering has been reported for other high-*k* dielectrics [17].

Next we present the results obtained for the case of Al metal gate / Al_2O_3 dielectric / $In_{1-x}Ga_xAs$ substrate. A 8 nm thick Al_2O_3 was atomic-layer-deposited on $In_{0.75}Ga_{0.25}As$ substrate, and subsequently subjected to post-deposition annealing (*PDA*) at 650 °C and 600 °C for 30 s [12]. A 12 nm thick Al layer of 100 μm × 100 μm size was then deposited on top of Al_2O_3 by thermal evaporation. IPE measurements were performed on these MOS structure with the bias applied to the substrate from −2.0 V to +2.0 V in steps of 0.1 V. As a reference, the pseudo-dielectric functions of $In_{0.75}Ga_{0.25}As$ and Al_2O_3, and the band gap of the Al2O3 film were determined by VUV-SE prior to the aluminum gate deposition. The dielectric function of Al_2O_3 is found to be essentially the same for all Al_2O_3 films; i.e., optically unaffected by the high temperature annealing up to 650 °C. In Fig. 5 the Al_2O_3 optical band gap of 6.8 eV was determined by the Tauc–Plot which shows a linear dependence of the $[n(E)\alpha(E)E]^{1/2}$ with the photon energy (E) near the band gap (E_g). The band gap is slightly larger than a similar study of band offset of Al_2O_3 on GaAs [18]. It has been suggested that the difference is largely due to the deposition or growth conditions which results in different atomic density. For instance, in a recent theoretical study, it was shown that amorphous Al_2O_3 having lower Al coordination numbers than that of Al atoms in α-Al_2O_3 has a narrower band gap relative to the crystal Al_2O_3 [19]. Fig. 6a shows the imaginary part (<ε_2>) of the pseudo-dielectric function of $In_{0.75}Ga_{0.25}As$ obtained from the VUV-SE measurement. Indicated in Fig. 6a are the three critical points E_1, $E_1+\Delta_1$, and E_2 in Brillouin zone where the E_2 structures consist of three broad and overlapped E_0', $E_0'+\Delta_0'$, and E_2. Reductions in the photocurrent are seen at the plateau regions on the IPE yield spectra between 2.4 eV and 2.8 eV and between 4.5 eV and 4.8 eV (Fig. 6b). Similar to the case of Si substrate above, the reduction at E_2 is due to the strong absorption or the decreasing light penetration depth and the X_5 critical point final state of the E_2 transition in the X crystal momentum direction being well below the Al_2O_3 bottom conduction band. $Y^{1/3}-h\upsilon$ plots, shown in Fig. 6b,

measured at an externally applied substrate bias of −2.0 V, clearly indicate that *PDA* samples have a lower energy threshold than those of as-deposited samples. The spectral thresholds ($\Phi_e^{'}$s) extracted by linear fits correspond to IPE from the InGaAs valence band maximum to the Al_2O_3 conduction band minimum. A redshift of about 0.3 eV is observed for all annealed samples with respect to the as-deposited samples. A similar shift was previously reported when GaAs surface conditions were treated and/or passivated [18], leading us to speculate that, the shift may be caused by the interfacial chemical modification. Another significant observation is the sub-threshold IPE signals as indicated by Φ_{int} in Fig. 6b. This could be due to the formation of an interlayer between the substrate and Al_2O_3. Similar sub-threshold photoemission has been shown to originate from an intentionally grown interlayer between the III–V substrates and the Al_2O_3 and HfO_2 gate dielectrics [20].

Under positive bias, photocurrents injected from the Al to Al_2O_3 for both *as-deposited* and *post-deposit annealed* samples show a rather insensitive response to the applied bias variation, meaning a rather weak field dependence of the barrier height at the Al and Al_2O_3 interface. The spectral thresholds (Φ_e) were determined by fitting the conventional Fowler plots ($Y^{1/2}$-$h\upsilon$, not shown). A rather weak dependence of the barrier heights on the Al_2O_3 electric field at the Al/Al_2O_3 interface is observed for both samples. The averaged *zero*-field barrier heights were found at three different values (3.0 eV ± 0.05 eV, 2.8 eV ± 0.05 eV, and 2.6 eV ± 0.05 eV). Such variation has been widely observed and speculated as the result of differences in atomic density of Al_2O_3 (see Fig. 1 in Ref. [3]). Since the Al_2O_3 surface was exposed to air ambient for a long period of time prior to Al deposition, it is quite probable that the contamination (i.e., adsorption of water) may contribute to the variation, as it is well known that the Al/ Al_2O_3 electronic interface properties are strongly dependent on growth and surface condition. In fact, metal/high-κ oxide interface barriers that have been measured show a strong sensitivity to the chemical nature at the interface [3].

Fig. 7 displays the Schottky plots of the Al_2O_3 electric field dependence of the barrier heights (Φ_e) at the Al_2O_3/ InGaAs interface. Φ_e at each applied bias was extracted from a linear fit to within 1 eV above the threshold using $Y^{1/3}$ -$h\upsilon$ plots. Within 0.1 eV uncertainties, the *zero*-field barrier heights (Φ^0_e) of *as-deposited* and *PDA* Al_2O_3 on $In_{0.75}Ga_{0.25}As$ substrates are 3.30 eV and 2.95 eV, respectively. Therefore it is concluded that the effect of *PDA* is to reduce the barrier height by 0.35 eV which is also clearly seen as a redshift of the quantum yield shown in Fig. 6. From the band gap of 0.55 eV of $In_{0.75}Ga_{0.25}As$, we conclude that the conduction band offset is 2.75 eV and 2.40 eV for *as-deposited* and *PDA* Al_2O_3, respectively. From the Al_2O_3 band gap of 6.80 eV measured by VUV-SE, the valence band offset becomes 3.50 eV and 3.85 eV for *as-deposited* and *PDA* Al_2O_3, respectively. Fig. 7 also shows that the *zero*-field barrier height of the interlayer was averaged to a value of 2.2 eV ± 0.3 eV. The annealing effect and the existence of the interlayer appear to degrade the current-voltage characteristics as we find that ALD Al_2O_3 have higher leakage currents than that of as-deposited samples (not shown). Finally, with the conduction band offset larger than 1.0 eV as required [21], ALD Al_2O_3 should be a suitable dielectric to use in a high mobility MOS device as long as the formation of the interlayer of lower barriers can be avoided, and the chemistry of the starting substrate surface must be well controlled to achieve stable and reliable devices [22].

Fig. 8 schematically summarizes the band alignment of the two structures discussed above. With the Si band gap of 1.12 eV and SiO_2 of 9.0 eV, from the measured barrier height of 4.3 eV, the band offsets, ΔE_c and ΔE_v, are 3.18 eV ± 0.1 eV and 4.7 eV ± 0.1 eV, respectively. For Al / Al_2O_3 / $In_{0.75}$ $Ga_{0.25}As$, the band offsets are influenced by the post deposition high temperature annealing. With the band gap of 6.8 eV and 0.55 eV of Al_2O_3 and $In_{0.75}$ $Ga_{0.25}As$, respectively, we found ΔE_c = 2.40 eV and ΔE_v = 3.85 eV for *PDA* Al_2O_3, and ΔE_c = 2.75 eV and ΔE_v = 3.50 eV for *as-deposited* Al_2O_3.

5. Conclusion

In this paper, we have presented an important combination of internal photoemission (IPE) and vacuum ultraviolet spectroscopic ellipsometry (VUV-SE) as a tool to enable the determination of band offset, thus the band alignment, of metal oxide semiconductor (MOS) device. A brief description of IPE was given with a focus on the spectral threshold spectroscopy aspect of this technique. Two technologically important classes of MOS that were studied to determine their band alignments are: [TaN/TaSiN] metal gate / [SiO_2/HfO_2] dielectric stack / Si substrate and Al metal gate / Al_2O_3 dielectric / $In_{1-x}Ga_xAs$ substrate. With the barrier heights determined by IPE and the band gaps determined by VUV-SE, we were able to establish the band alignments for both structures. For the case of Al metal gate / Al_2O_3 dielectric / $In_{1-x}Ga_xAs$, we also observed the existence of the interlayer between the Al_2O_3 layer and $In_{1-x}Ga_xAs$ substrate giving rise to the photocurrent sub-barrier threshold.

Acknowledgement

The authors gratefully acknowledge funding from the NIST Office of Microelectronics Programs.

References

[1] P.D. Ye, IEEE Spectr. 45 (2008) 42.
[2] G.D. Wilk, R.M. Wallace, J.M. Anthony, J. Appl. Phys. 89 (2001) 5243.
[3] V.V. Afanas'ev, A. Stesmans, J. Appl. Phys. 102 (2007) 28.
[4] V.V. Afanas'ev, Internal Photoemission Spectroscopy: Principles and Applications, Elsevier, Amsterdam, 2008.
[5] T.H. Distefano, J. Vacuum Sci. Technol. 13 (1976) 856.
[6] R.H. Fowler, Phys. Rev. 38 (1931) 45.
[7] R.J. Powell, J. Appl. Phys. 41 (1970) 2424.
[8] S.M. Sze, Physics of Semiconductor Devices, John Wiley & Sons, Inc., New Jersey, 1981.
[9] N.V. Nguyen, A.V. Davydov, D. Chandler-Horowitz, M.M. Frank, Appl. Phys. Lett. 87 (2005) 192903.
[10] N.V. Nguyen, S. Sayan, I. Levin, J.R. Ehrstein, I.J.R. Baumvol, C. Driemeier, C. Krug, L. Wielunski, R.Y. Hung, A. Diebold, J. Vac. Sci. Technol., A 23 (2005) 1706.
[11] N.V. Nguyen, H.D. Xiong, J.S. Suehle, O.A. Kirillov, E.M. Vogel, P. Majhi, H.C. Wen, Appl. Phys. Lett. 92 (2008) 92907.
[12] N.V. Nguyen, M. Xu, O.A. Kirillov, P.D. Ye, C. Wang, K. Cheung, J.S. Suehle, Appl. Phys. Lett. 96 (2010) 52107.
[13] M.C. Cheynet, S. Pokrant, F.D. Tichelaar, J.L. Rouviere, J. Appl. Phys. 101 (2007) 54101.
[14] S.G. Lim, S. Kriventsov, T.N. Jackson, J.H. Haeni, D.G. Schlom, A.M. Balbashov, R. Uecker, P. Reiche, J.L. Freeouf, G. Lucovsky, J. Appl. Phys. 91 (2002) 4500.
[15] V.V. Afanas'ev, M. Houssa, A. Stesmans, M.M. Heyns, Appl. Phys. Lett. 78 (2001) 3073.
[16] V.V. Afanas'ev, A. Stesmans, F. Chen, X. Shi, S.A. Campbell, Appl. Phys. Lett. 81 (2002) 1053.
[17] V.V. Afanas'ev, M. Houssa, A. Stesmans, M.M. Heyns, J. Appl. Phys. 91 (2002) 3079.
[18] N.V. Nguyen, O.A. Kirillov, W. Jiang, W. Wang, J.S. Suehle, P.D. Ye, Y. Xuan, N. Goel, K.W. Choi, W. Tsai, S. Sayan, Appl. Phys. Lett. 93 (2008) 82105.
[19] H. Momida, T. Hamada, Y. Takagi, T. Yamamoto, T. Uda, T. Ohno, Phys. Rev. B 73 (2006) 54108.
[20] V.V. Afanas'ev, M. Badylevich, A. Stesmans, G. Brammertz, A. Delabie, S. Sionke, A. O'Mahony, I.M. Povey, M.E. Pemble, E. O'Connor, P.K. Hurley, S.B. Newcomb, Appl. Phys. Lett. 93 (2008) 212104.
[21] J. Robertson, B. Falabretti, J. Appl. Phys. 100 (2006) 14111.
[22] C.L. Hinkle, M. Milojevic, E.M. Vogel, R.M. Wallace, Microelectron. Eng. 86 (2009) 1544.